

## Surface order reconstruction in nematics

H. Ayeb,<sup>1,2</sup> G. Lombardo,<sup>3</sup> F. Ciuchi,<sup>3</sup> R. Hamdi,<sup>1</sup> A. Gharbi,<sup>2</sup> G. Durand,<sup>4</sup> and R. Barberi<sup>1,3,a)</sup>

<sup>1</sup>Department of Physics, University of Calabria, Ponte Pietro Bucci, 87036 Rende, Italy

<sup>2</sup>Département de Physique, Laboratoire de Physique de la Matière Molle, Faculté des Sciences de Tunis, Université de Tunis El Manar, 2092 Tunis, Tunisia

<sup>3</sup>CNR-IPCF Licryl, c/o University of Calabria, Ponte Pietro Bucci, 87036 Rende, Italy

<sup>4</sup>Laboratoire de Physique des Solides associé au CNRS (LA2), Université Paris Sud, 91405 Orsay, France

(Received 4 March 2010; accepted 13 May 2010; published online 8 September 2010)

Investigations on  $\pi$ -cell, a sandwich cell with the director rotating by  $180^\circ$ , demonstrate the possibility to obtain nematic transitions between two textures with different topologies, for instance between an untwisted state and a  $\pi$ -twisted one. These fast textural changes can be obtained by bulk order reconstruction, which allows the director reorientation between two perpendicular directions without macroscopic rotations of the director itself, or by anchoring breaking, which transforms a weak planar anchoring in a homeotropic surface state. Now, we demonstrate that order reconstruction close to a boundary surface with strong or infinite anchoring conditions provides transitions equivalent to anchoring breaking. © 2010 American Institute of Physics.

[doi:10.1063/1.3455885]

Electro-optical experiments on nematic liquid crystals are often carried out using sandwich cells with two transparent flat plates containing a micrometric film of nematic material. A  $\pi$ -cell is a sandwich cell in which the director can rotate by  $180^\circ$  through the cell. More than ten years ago a  $\pi$ -cell with weak anchoring energy has been used to observe and describe the anchoring breaking, which is a mechanism to achieve fast textural transitions in nematics as follows: a uniform planar or splay texture is transformed in a  $\pi$ -twisted one, changing the starting topology, by breaking the nematic orientation on the surface with an electric pulse.<sup>1,2</sup> More recently, similar textural transitions have been achieved by using the bulk biaxial order reconstruction,<sup>3</sup> which is a mechanism also able to connect two nematic textures with distinct topologies.<sup>4-7</sup> Up to now, the nematic order reconstruction has been studied as a pure bulk effect but it is known that surface properties can influence its behavior.<sup>8,9</sup> As the electrically controlled anchoring breaking requires weak anchoring conditions,<sup>1,2</sup> while bulk order reconstruction can work with strong anchoring,<sup>3</sup> it is intriguing to explore what can happen when the order reconstruction occurs close to a boundary surface and this work presents a comparison between surface nematic biaxial order reconstruction and anchoring breaking.<sup>5-7</sup>

Biaxial order reconstruction is usually achieved using a symmetric splay texture  $H$  that is transformed in a topologically distinct  $\pi$ -bent configuration  $B$  (or  $\pi$ -twisted state  $T$  as bend and twist have the same topology).<sup>3</sup> In the symmetric case, a planar wall is located in the middle of the cell, but, if the nematic pretilt orientations on the two boundary surfaces are not symmetric, the planar wall is close to the surface with smaller pretilt.<sup>2,10,11</sup>

To experimentally investigate  $H$ - $B$  transitions, sandwich  $\pi$ -cells are made with two parallel transparent indium tin oxide (ITO) coated glasses plates, which are filled with 4-cyano-4'-n-pentylbiphenyl (5CB), a nematic with strong

positive dielectric anisotropy [ $\epsilon_a \approx 12$  at  $25^\circ\text{C}$  (Ref. 12)]. Electrodes are made by photolithographic treatment of the ITO film on the two plates: the etching stripes are 1 mm wide and their crossed superposition gives one pixel of about  $1\text{ mm}^2$  area.

We prepared three different cells having different surface anchoring treatments as follows: one symmetric cell (SC1) and two asymmetric cells (AC1 and AC2). SC1 presents symmetrical surface aligning layers on both plates, while AC1 and AC2 present asymmetrical aligning layers. The SC1 aligning layers are both made by using a mixture of 20% weight of polyimide (PI) in pyrrolidinone, obtaining a film thickness of about 50 nm, which is rubbed, giving a pretilt of about  $8^\circ$ . AC1 and AC2 have one aligning surface layer identical to SC1, while the other one is made with a different mixture of PI in pyrrolidinone; 10% and 2% for AC1 and AC2, respectively. This second aligning layer has a thickness of 20 nm with a pretilt of  $6^\circ$  for AC1 and a thickness of 6 nm with a pretilt of  $2^\circ$  for AC2. Using a standard interferential method,<sup>13,14</sup> we measured the zenithal anchoring strengths which result as  $2.5 \times 10^{-4}\text{ J/m}^2$ ,  $2 \times 10^{-4}\text{ J/m}^2$ , and  $1 \times 10^{-4}\text{ J/m}^2$ , in the same order of magnitude, for 20%, 10%, and 2% of PI in pyrrolidinone, respectively. As these values of surface anchoring energies are strong, we do not expect to observe anchoring breaking phenomena.

Each cell is placed in a temperature controlled oven and it is observed by means of a polarizing microscope. The upper and lower electrodes of each sample are connected to a pulse generator and the  $H$ - $B$  textural transition is obtained by applying a rectangular electric pulse. Figure 1 shows the dependence of the electric transition threshold  $E_{th}$  on the pulse width  $\tau$  for SC1, AC1, and AC2 at  $T=30^\circ\text{C}$ . The three cells present similar behaviors. The highest threshold values are observed for the symmetric cell SC1 while the lowest ones for the less symmetric cell AC2. In all cases, the electric field is strong enough to concentrate the nematic distortion over an electric coherence length, which is comparable with the nematic coherence length.<sup>15</sup> In this situation, the nematic

<sup>a)</sup>Electronic mail: riccardo.barberi@fis.unical.it.

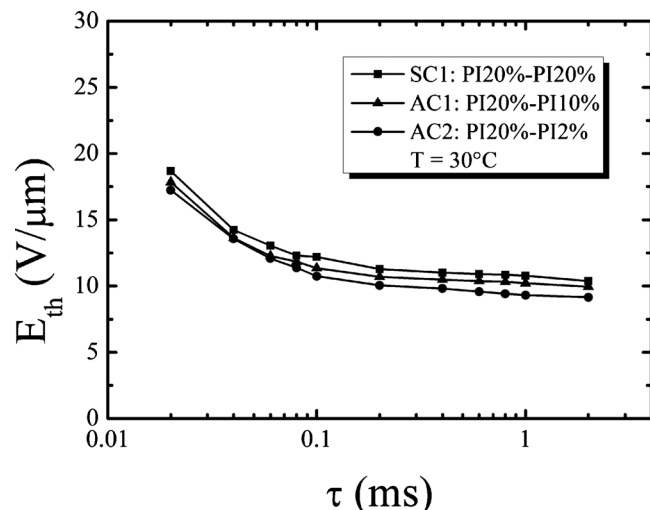


FIG. 1.  $H$ - $B$  transition threshold  $E_{th}$  vs pulse duration  $\tau$  at  $T=30$  °C for the three cells SC1, AC1, and AC2.

order may be significantly altered, as in the case of the core of a defect<sup>16</sup> or in the case of highly frustrated nematic systems.<sup>9</sup> Now order gradients and local biaxiality become important and a tensorial representation of nematic order is required.<sup>17,18</sup>

In order to catch how the nematic distortion evolves, we model the  $\pi$ -cell with a one-dimensional domain of thickness  $1 \mu\text{m}$ , with an applied electric field perpendicular to boundaries with infinite anchoring energy. We also fix the temperature  $T_C - T = 3$  °C ( $T_C$  is the nematic-isotropic transition temperature). The  $H$ - $B$  transition is described in terms of the order tensor  $\mathbf{Q}$ , whose eigenvectors give the directions of the preferred molecular orientation and whose eigenvalues give the degree of order along these directions. The  $\mathbf{Q}$ -dynamics is expressed by a balance between the Rayleigh dissipation function and the rate of change in the free energy.<sup>3</sup> The total free energy,<sup>15</sup> sum of thermotropic, distortion and electrostatic terms, is calculated by using a finite element method. The explicit form of each term as well as a detailed description of the minimization numerical procedure can be found in Ref. 17.

Starting from the temporal evolution of the  $\mathbf{Q}$  configuration, we calculate the director field and the scalar order parameter dynamics inside the cell. Moreover we compute the biaxiality  $\beta = (1 - 6((\text{tr } \mathbf{Q}^3)^2 / (\text{tr } \mathbf{Q}^2)^3))^{0.5}$ , which is a convenient parameter to show spatial inhomogeneities of  $\mathbf{Q}$ .<sup>3</sup> The temporal evolution of  $\beta$  for the  $H$ - $B$  transition inside a symmetric  $\pi$ -cell is reported in Ref. 17. The starting quasi-planar director tends to realign along the vertical electric field everywhere inside the cell except near the surface layers and in the center of the domain, where the maximum nematic distortion is concentrated and a biaxial region of thickness comparable with the biaxial coherence length grows.<sup>6</sup> This dynamical behavior is analogous to the spatial order variation, which occurs around the core of a nematic defect.<sup>16</sup> The textural transition from  $H$  to  $B$  is completed after a few tens of microseconds.

Figure 2 represents the dynamics of the nematic biaxiality inside an asymmetric  $\pi$ -cell. The pretilt angles on the upper surface and on the lower surface are  $-19^\circ$  and  $+1^\circ$ , respectively. Applying a strong enough electric field at  $t=0$  s, the nematic distortion is now concentrated very close

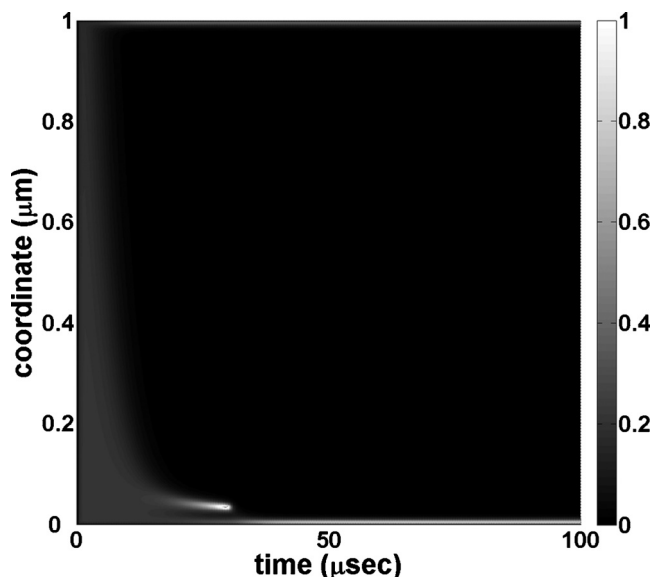


FIG. 2. Numerical simulation of space-time evolution of the biaxiality  $\beta$  in the case of an asymmetric  $\pi$ -cell (white for  $\beta=1$ , black for  $\beta=0$ , and gray scale for intermediate values).

to the bottom boundary surface. Also in this case, only about  $30 \mu\text{s}$  are enough to complete the textural transition from  $H$  to  $B$ . The thin biaxial layer, which connects the planar region with the bent nematic textures, is so close to the bottom boundary surface that, in practice, it behaves as the surface anchoring breaking, which transforms a planar anchoring in a homeotropic state. The main difference is that anchoring breaking requires a uniform weak anchoring, which is not easy to be achieved on real samples, whereas our experiments are made with strong anchoring conditions and they can be interpreted in terms of a pure bulk effect; the nematic order reconstruction.

For a better understanding of these phenomena, we prepared two other asymmetrical  $\pi$ -cells in order to assembly samples with an aligning treatment previously used to observe surface anchoring breaking effects. Both AC3 and AC4 use 5CB and are made with a plate treated with  $\text{SiO}_x$  evaporation to obtain a planar aligning surface layer with weak anchoring energy conditions,<sup>1</sup> the same used for surface anchoring breaking observations,<sup>2</sup> whereas the second plate is treated to give a large pretilt, obtained with a mixture of 20% PI in pyrrolidinone for AC3 and by a different  $\text{SiO}_x$  evaporation for AC4.<sup>19</sup> Figure 3 shows the comparison of electric  $H$ - $B$  textural transition thresholds for all samples, SC1, AC1, AC2, AC3, and AC4, and also the surface anchoring breaking electric threshold curve presented in Ref. 1 for 5CB. Moreover we obtained similar  $H$ - $B$  transitions for 5CB in asymmetric cells where a planar anchoring is given by rubbed films of polyvinyl alcohol (PVA), which is well known to produce very strong anchoring and these further data are also reported in Fig. 3. All these samples exhibit comparable threshold fields, with similar behaviors that seem to be due to a unique phenomenon not strictly related with anchoring energy, but rather with some material property.

As it is known that doping a pure calamitic nematic as 5CB with suitable molecules it is possible to control the biaxial coherence length and hence the electric threshold for the bulk order nematic reconstruction, in order to check if the transition which occurs in asymmetric  $\pi$ -cells is due to a

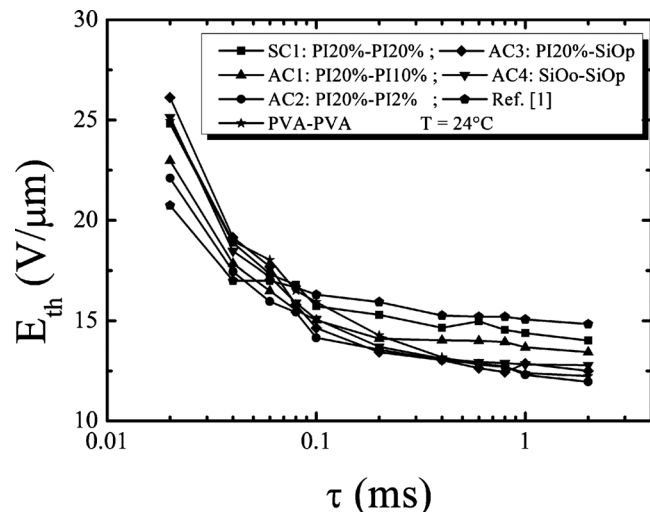


FIG. 3.  $H$ - $B$  transition threshold  $E_{th}$  vs pulse duration  $\tau$  at  $T=24^\circ\text{C}$  for cells SC1, AC1, AC2, AC3, AC4, and with PVA compared with experimental data of Ref. 1.

pure bulk effect instead of a surface effect, we filled an asymmetric  $\pi$ -cell AC2 with a mixture containing 5CB and a concentration in weight of 2% of  $n$ -4'-methoxybenzylidene- $n$ -butylanilin (MBBA) from Merck as in Ref. 6. Figure 4 shows the electric threshold versus the reduced temperature,  $T_c - T$ , at fixed  $\tau=1$  ms or  $\tau=0.1$  ms for this cell when filled with pure or doped 5CB. The doped material shows lower transition thresholds confirming that the fast  $H$ - $B$  transition in an asymmetric  $\pi$ -cell with strong anchoring is related with bulk nematic order reconstruction.

All experimental data of symmetric and asymmetric  $\pi$ -cells present similar electro-optical behaviors and the control of the biaxial coherence length and hence of the electric threshold, both in symmetric and asymmetric  $\pi$ -cells, indi-

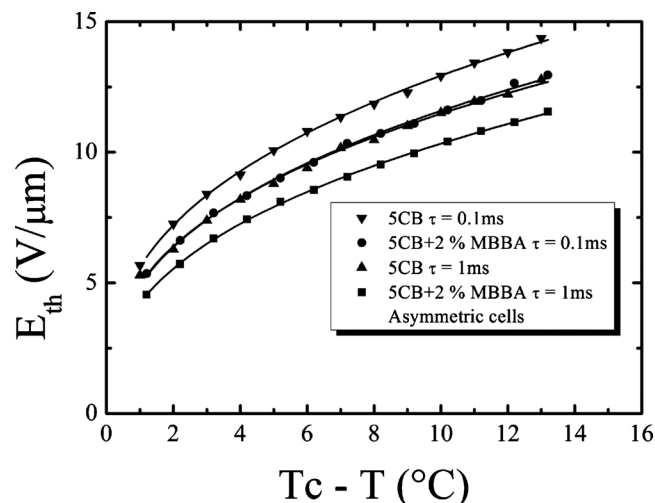


FIG. 4.  $H$ - $B$  transition threshold  $E_{th}$  vs reduced temperature for an asymmetric  $\pi$ -cell filled with pure or doped 5CB for  $\tau=1$  ms or  $\tau=0.1$  ms.

cates that the  $H$ - $B$  transition mainly depends on bulk nematic properties, without relevance if it happens close or far from a boundary surface or in presence of weak or strong anchoring. Moreover, the proposed biaxial dynamical model<sup>17</sup> captures the relevant physical aspects related with all experimental observations. A strong electric field in an asymmetric cell induces a strong nematic distortion near the boundary surface with smaller pretilt and the strain is relaxed by lowering the nematic order through biaxial states. The two competing nematic orientations, i.e., the orientation imposed by the surface layer and the other one given by the electric field, are now bridged by a thin biaxial surface wall as in Fig. 2. The net macroscopic result is that the topological transition between  $H$  and  $B$  textures is allowed also very close to a boundary surface without the need of anchoring breaking.

This result is also relevant for applications. In fact, all actual developments of bistable nematic displays require special surface treatments to achieve one kind of  $H$ - $B$  transition,<sup>20-23</sup> but the biaxial order reconstruction is expected to play a relevant role and should be carefully taken into account.

<sup>1</sup>I. Dozov, M. Nobili, and G. Durand, *Appl. Phys. Lett.* **70**, 1179 (1997).

<sup>2</sup>I. Dozov and P. Martinot-Lagarde, *Phys. Rev. E* **58**, 7442 (1998).

<sup>3</sup>R. Barberi, F. Ciuchi, G. Durand, M. Iovane, D. Sikharulidze, A. Sonnet, and E. Virga, *Eur. Phys. J. E* **13**, 61 (2004).

<sup>4</sup>P. Martinot-Lagarde, H. Dreyfus-Lambe, and I. Dozov, *Phys. Rev. E* **67**, 051710 (2003).

<sup>5</sup>R. Barberi, F. Ciuchi, G. Lombardo, R. Bartolino, and G. Durand, *Phys. Rev. Lett.* **93**, 137801 (2004).

<sup>6</sup>F. Ciuchi, H. Ayeb, G. Lombardo, R. Barberi, and G. E. Durand, *Appl. Phys. Lett.* **91**, 244104 (2007).

<sup>7</sup>H. Ayeb, F. Ciuchi, G. Lombardo, and R. Barberi, *Mol. Cryst. Liq. Cryst.* **481**, 73 (2008).

<sup>8</sup>G. Lombardo, H. Ayeb, F. Ciuchi, M. P. De Santo, R. Barberi, R. Bartolino, E. G. Virga, and G. E. Durand, *Phys. Rev. E* **77**, 020702 (2008).

<sup>9</sup>G. Carbone, G. Lombardo, R. Barberi, I. Musevic, and U. Tkalec, *Phys. Rev. Lett.* **103**, 167801 (2009).

<sup>10</sup>H. Nakamura and M. Noguchi, *Jpn. J. Appl. Phys., Part 1* **39**, 6368 (2000).

<sup>11</sup>B. Wang, Y. Zhang, Y. K. Jang, and P. J. Bos, *Jpn. J. Appl. Phys.* **48**, 022502 (2009).

<sup>12</sup>B. Ratna and R. Shashidhar, *Mol. Cryst. Liq. Cryst.* **42**, 113 (1977).

<sup>13</sup>T. J. Scheffer and J. Nehring, *J. Appl. Phys.* **48**, 1783 (1977).

<sup>14</sup>S. Palto, R. Barberi, M. Iovane, V. V. Lazarev, and L. Blinov, *Mol. Cryst. Liq. Cryst. Sci. Technol., Sect. C, Molecular Materials* **11**(4), 277 (1999).

<sup>15</sup>P. G. de Gennes and J. Prost, *The Physics of Liquid Crystals*, 2nd ed. (Clarendon, Oxford, 1993).

<sup>16</sup>N. Schopohl and T. J. Sluckin, *Phys. Rev. Lett.* **59**, 2582 (1987).

<sup>17</sup>G. Lombardo, H. Ayeb, and R. Barberi, *Phys. Rev. E* **77**, 051708 (2008).

<sup>18</sup>S. Kralj, R. Rosso, and E. G. Virga, *Phys. Rev. E* **81**, 021702 (2010).

<sup>19</sup>M. Monkade, M. Boix, and G. Durand, *Europhys. Lett.* **5**, 697 (1988).

<sup>20</sup>M. Giocondo, I. Lelidis, I. Dozov, and G. Durand, *Eur. Phys. J.: Appl. Phys.* **5**, 227 (1999).

<sup>21</sup>J. Cliff Jones, *SID Int. Symp. Digest Tech. Papers* **38**, 1347 (2007).

<sup>22</sup>L. A. Parry-Jones, E. G. Edwards, S. J. Elston, and C. V. Brown, *Appl. Phys. Lett.* **82**, 1476 (2003).

<sup>23</sup>A. Majumdar, C. J. P. Newton, J. M. Robbins, and M. Zyskin, *Phys. Rev. E* **75**, 051703 (2007).